THE JOURNAL OF PHYSICAL CHEMISTRY C
A JOURNAL OF THE AMERICAN CHEMICAL SOCIETY

pubs.acs.org/JPCC

Article

Gas-Phase Hydrogen-Atom Measurement above Catalytic and Noncatalytic Materials during Ethane Dehydrogenation

Scott A. Steinmetz, Andrew T. DeLaRiva, Christopher Riley, Paul Schrader, Abhaya Datye, Erik D. Spoerke,* and Christopher J. Kliewer*

Cite This: *J. Phys. Chem. C* 2022, 126, 3054−3059

Read Online

ACCESS | Metrics & More | Article Recommendations

ABSTRACT: The role of a solid surface for initiating gas-phase reactions is still not well understood. The hydrogen atom (H) is an important intermediate in gas-phase ethane dehydrogenation and is known to interact with surface sites on catalysts. However, direct measurements of H near catalytic surfaces have not yet been reported. Here, we present the first H measurements by laser-induced fluorescence in the gas-phase above catalytic and noncatalytic surfaces. Measurements at temperatures up to 700 °C show H concentrations to be at the highest above inert quartz surfaces compared to stainless steel and a platinum-based catalyst. Additionally, H concentrations above the catalyst decreased rapidly with time on stream. These newly obtained observations are consistent with the recently reported differences in bulk ethane dehydrogenation reactivity of these materials, suggesting H may be a good reporter for dehydrogenation activity.

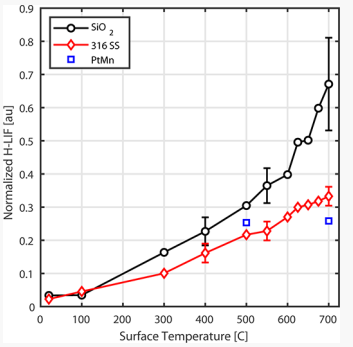

1. INTRODUCTION

Understanding the interactions between heterogeneous catalysts and the gas-phase poses a significant scientific challenge. While the nature of adsorbed species on a catalytic surface can be studied using various analytical methods, less is known about the gas phase, especially the concentration of short-lived radical species. These species become important during the study of reactions such as ethane dehydrogenation, where gas phase reactions can dominate over surface reactions at elevated temperatures. The local chemistry can vary spatially due to differences in gas-phase composition, active site availability, temperature, and pressure. The conventional approach for the study of heterogeneous catalysts involves a study of catalyst performance through analysis of downstream products, for example, by detailed speciation with gas chromatography (GC).[1] Studies of catalyst surfaces are often done at low pressures using surface science tools since these conditions, however unrealistic, provide simpler, more easily characterized systems. Bridging the so-called "pressure gap" has been critical to catalyst development.[2] The need for improved characterization of catalyst surfaces, their active sites, and their surface chemistry at relevant conditions has led to significant development of operando diagnostics.[3] While surface diagnostics under realistic conditions have received much attention, there have been limited in situ studies of the gas-phase and its interaction with catalysts, despite its importance. Here, we use laser-induced fluorescence (LIF) as a tool to explore local hydrogen atom (H) production over surfaces, applying the process to the characterization of industrially important ethane dehydrogenation reactions.

Rosén and co-workers used LIF to measure OH radical over Pt during hydrogen oxidation.[4−8] Zetterberg and co-workers have done significant work combining in situ LIF in the gas-phase with high energy X-ray diffraction and surface optical reflectance to study catalytic CO oxidation.[9−20] Deutschmann and co-workers have used local gas sampling[21] and LIF[22,23] to study catalytic oxidation and reduction reactions. Most recently, Zhou et al.[24] have combined LIF, Raman, and near-surface MS to characterize a catalytic methanol oxidation system. In each of these studies, key gas-phase species serve as local reporters of catalytic activity. These studies show that the application of near-surface gas-phase measurements can be an invaluable tool for catalyst development. The current work seeks to extend this concept to an alkane dehydrogenation system.

Olefins are important chemicals in a number of industries. In order to meet growing demands, dehydrogenation of alkanes (e.g., ethane) as a route to industrial alkenes (e.g., ethylene) has received significant attention.[25,26] Currently, high-temperature (850−900 °C), energy-intensive steam cracking is the most common method of ethane dehydrogenation.[26] However, catalytic alternatives have also been the focus of significant

Received: November 20, 2021
Revised: January 20, 2022
Published: February 2, 2022

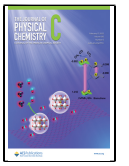

research,[1,26,27] seeking to reduce the energy requirement of the dehydrogenation process, typically through reduced operating temperatures. A significant challenge in catalyst development is suppression of side reactions, which can often lead to contamination of the catalyst, and numerous additives are being explored.[25,26]

A recent study by Riley et al. demonstrated high ethylene yield at reduced temperatures, but without catalyst, through ethane dehydrogenation in a quartz tube reactor.[28] The thermally driven reaction avoids the problems of catalyst contamination and regeneration, while significantly reducing operating temperatures to 700 °C. The authors note that the introduction of catalyst reduced reactor performance at this temperature. Additionally, a quartz tube reactor outperformed a stainless steel reactor.[28] Understanding the nature of these differences, however, is difficult using traditional bulk effluent analysis, such as GC-FID/TCD. Here, we explore LIF as a method to characterize local gas-phase measurements near the reactor and catalyst surfaces, potentially providing additional insight into this promising reactor system.

Dehydrogenation or pyrolysis of ethane involves a number of important radical species, such as methyl (CH_3) and H.[29,30] The importance of H in dehydrogenation makes it an attractive candidate as a gas-phase reporter of dehydrogenation chemistry. Additionally, hydrogen abstracted on reactive sites on a catalyst can "spillover" onto inactive sites on the substrate.[31] This surface-bound H can participate in surface-based reactions, including the formation of H_2. However, the transport of this H into the gas-phase and participation in gas-phase reactions is still not well understood. Baumgarten and co-workers[32−37] indirectly observed gas-phase H atom transport through the measurement of detector species or reaction products downstream. To our knowledge, no direct measurement of H in the gas-phase has been made near a catalytic surface.

The purpose of this study was to investigate H concentration in the gas-phase near catalytic and noncatalytic surfaces during ethane dehydrogenation. This is accomplished by three-photon LIF. Idealized surfaces are investigated in a stagnation reactor geometry in order to provide a well-characterized flow field and well-controlled temperature.

2. MATERIALS AND METHODS

Stainless steel and quartz samples were commercially obtained (Goodfellow). The steel is 316 stainless and is in the form of 0.5 mm thick, 10 mm diameter disks. The quartz (SiO_2) samples are 0.5 mm thick, 10 mm × 10 mm sheets. The catalyst contains platinum−manganese bimetallic nanoparticles supported on silica with nominal 2 wt % Pt loading (PtMn). The PtMn catalyst was prepared according to the procedure used by Wu et al.[38] using sequential incipient wetness of pH-adjusted manganese(II) nitrate solution and tetraamine platinum nitrate solution. The catalyst has been characterized via X-ray diffraction (XRD), X-ray fluorescence (XRF), Brunauer−Emmett−Teller (BET) surface area analysis, and transmission electron microscopy (TEM).[28] XRD analysis determined the crystalline phases present within the Pt-based catalyst and was conducted with a Bruker D2 Phaser operating in Bragg−Brentano geometry. XRF elemental composition measurements were taken with an Orbis Micro-XRF using a 30 μm spot size, a 20 kV voltage, and an 800 μA current. Surface area measurements were taken with a Micromeritics Gemini 2360 surface area analyzer. Samples were outgassed overnight at 120 °C in flowing nitrogen prior to analysis. A JEOL JEM 2010 F field emission microscope was used for TEM imaging. Surface characterization results can be found in the Supporting Information of ref 28. The catalyst powder was formed into 1 mm thick, 6.35 mm diameter pellets with a press (Retsch PP 25, 1000 MPa pellet pressure).

Samples were placed in a vacuum-capable stainless steel cell, as shown in Figure 1. Each side of the cell is equipped with 3

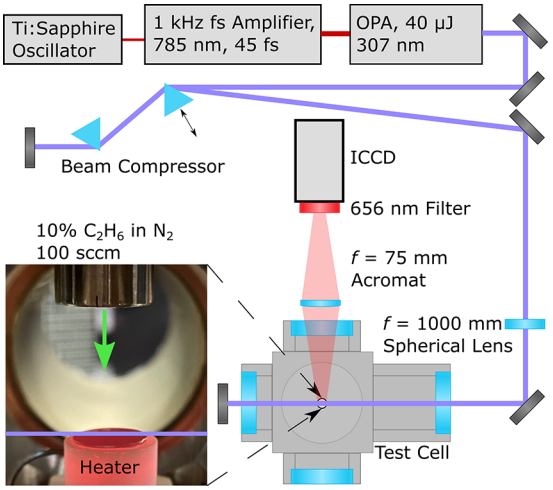

Figure 1. Test cell and LIF diagnostic.

mm thick UV-grade windows. A half-inch ceramic button heater (model 101275−28, HeatWave Labs) was used to heat materials to specified temperatures up to 700 °C. Measurements were limited to 700 °C as coke formation on heater leads would cause heater malfunction at higher temperatures. Reactants (controlled by mass flow controllers, MKS) flow into the cell from a 9.4 mm inner diameter tube and impinge on the heated material in a stagnation flow configuration. The outlet of the tube was a distance, h, of 20 mm from the heated material surface. The cell is vented to an exhaust stream, and all measurements are carried out at ambient pressure. The reactant stream was 10% ethane, by volume, with the balance as nitrogen. The total volumetric flow rate, Q, was 100 sccm (0 °C reference) to produce similar gas velocities to those in ref 28. Given the differences in system configurations, however, residence times cannot be directly matched, though the results of Riley et al.[28] showed limited sensitivity to residence time.

Hydrogen atom concentration was measured by femtosecond (fs) three-photon laser-induced fluorescence.[39] 307 nm radiation was produced by an Optical Parametric Amplifier (OPA, HE-TOPAS Prime, Light Conversion). The OPA was pumped by 8 mJ, 45 fs pulses at 1 kHz (Legend Elite Duo, Coherent). The 307 nm beam pulse energy was reduced by an ND filter to 40 μJ to limit plasma generation at the beam focus[39] and had a bandwidth of approximately 5 nm. The inherent and window-induced first-order chirp of the fs UV beam was compensated for with a two-prism compressor.

The UV beam was focused by a 1 m focal length lens to approximately 250 μm diameter, and the edge of the beam passed over the materials at a distance of less than 50 μm. The entire cell is mounted on a translation stage allowing the relative position between the surface and the fixed beam to be adjusted. Fluorescence was collected normal to the beam propagation direction by a 2-in., 75 mm focal-length acromatic doublet lens. Hydrogen atom excited by the 307 nm beam

https://doi.org/10.1021/acs.jpcc.1c09955
J. Phys. Chem. C 2022, 126, 3054−3059

fluoresces at 656 nm.[39] Collected LIF was passed through a 656 nm narrowband filter (656FS03-25, Andover). The lens imaged LIF to an intensified CCD with a third generation intensifier (iCCD, iStar, Andor). The intensifier gain was set to 75% and gated to 10 ns. Each image consists of 800 intensifier gates accumulated on-chip. A total of 100 images were averaged for each measurement. Background signals were acquired by removing ethane from the reactant stream.

A rich (equivalence ratio = 1.2) methane/air flame was used to reliably produce H for the purpose of system optimization and calibration. It should be noted that H-LIF intensities in these experiments are 2 orders of magnitude lower than those in the flame. Krypton gas, which has similar transition energies to H,[40] was also used as a measure of day-to-day performance of the system.

The presence of H was first confirmed by coupling the iCCD to a spectrometer (Shamrock 500i, Andor). The spectrally resolved LIF signal above SiO_2 at 700 °C is shown in Figure 2. With the narrowband filter removed, a peak in

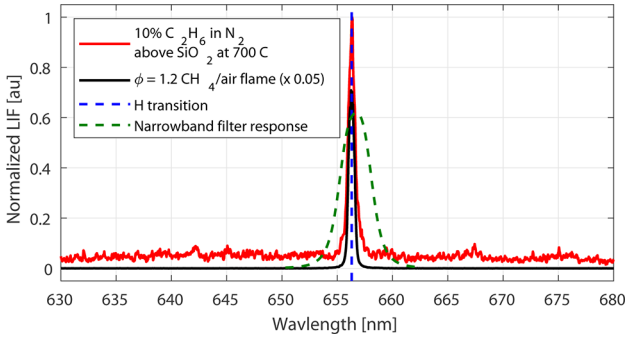

Figure 2. LIF spectrum.

fluorescence emissions is detected at 656 nm, confirming the presence of H. Figure 2 also shows the spectral response of the narrowband filter used in all H-LIF measurements. It is worth noting that there is some broadband LIF not associated with H collected at each condition. However, evaluation of the spectral response shown in Figure 2 provides an upper bound of this interference of about 5%.

The sensitivity of the system to h and Q was evaluated by comparing LIF signals over SiO_2 at 700 °C. These results are summarized in Figure 3. Negligible differences in H-LIF were found with h varying from 6 to 20 mm. An order of magnitude increase in Q from 100 to 1000 sccm, thereby decreasing residence time, reduced overall LIF signals by approximately 30%.

3. RESULTS AND DISCUSSION

Signals are integrated along the width of the beam and the length over the material. The signal for the C_2H_6/N_2 mixture is normalized by the signal in Kr to account for changes in laser energy or system response. It should be noted that the response in Kr was found to be insensitive to temperatures above 300 °C. It is assumed that the bulk gas composition above the different surfaces is comparable enough that there are negligible differences in quantum efficiency and fluorescence lifetime. With this assumption, H-LIF responses for different materials can be compared, and H-LIF intensities were assumed to be proportional to H number density. Measurements were made at successively increasing temperatures. Between each measurement, the cell was purged with

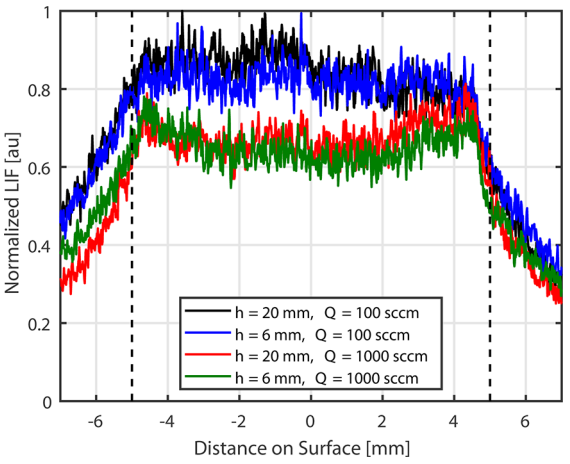

Figure 3. H-LIF above SiO_2 at 700 °C with reactant tube distances of 6 or 20 mm, and overall flow rates of 100 or 1000 sccm. Dashed lines indicate locations of the surface edge.

pure nitrogen for measurement of the background largely comprised of the heated surface blackbody radiation. Additionally, as the temperature is increased, small surface or beam position changes were tracked by measurements of LIF in krypton, and the surface was moved to keep a consistent measurement distance.

This technique was subsequently applied to assess H production and, thereby, ethane dehydrogenation, above several material surfaces. Normalized hydrogen-atom LIF signals over each of the materials are summarized in Figure 4. Error bars represent the standard deviation of repeat

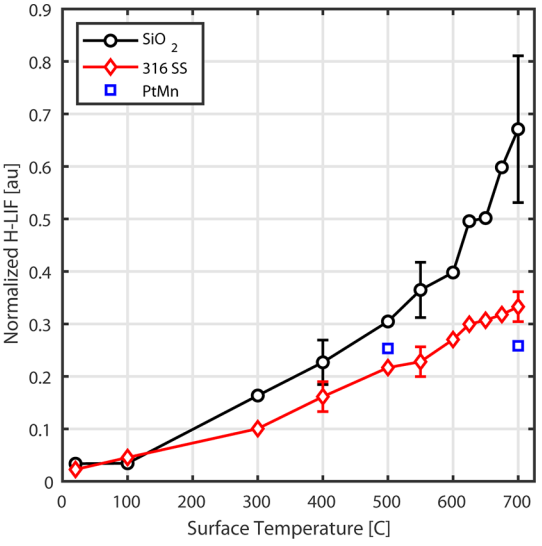

Figure 4. Normalized H-LIF above surfaces over a range of temperatures. Measurements are made 125 μm from the surface.

measurements combined in quadrature with the 5% uncertainty due to broadband interference. For both quartz and steel, increases in surface temperature result in increased H-LIF just above the surface. The increases are monotonic with temperature, consistent with a thermally driven production of H. Notably, the concentration of H above quartz is about a factor of 2 higher than stainless steel at 700 °C. This difference in H concentration is consistent with the higher fraction of bulk ethane conversion observed in a quartz

https://doi.org/10.1021/acs.jpcc.1c09955
J. Phys. Chem. C 2022, 126, 3054−3059

reactor, compared to a steel reactor.[28] It is worth noting no presence of coke deposition is observed on either quartz or steel over the entire temperature range.

Riley et al.[28] compared the performance of a blank quartz tube reactor to a system containing a PtMn catalyst. The PtMn catalyst performed relatively poorly at 700 °C, generating significant coking that was believed to degrade the catalyst performance. At lower temperatures (<600 °C), however, coking was less pronounced, and the catalyst outperformed the blank quartz tube at the same temperatures. The present LIF technique was therefore applied to explore potential local dehydrogenation above PtMn catalyst at 500 °C, where the catalyst is expected to outperform quartz, and 700 °C, where the quartz is expected to outperform the coking catalyst. Immediately before testing, the catalysts were reduced in 10% H_2 in N_2 at 400 °C for 1 h. Measurements for the catalyst are limited to two temperatures as coking and deactivation of the catalyst is a known problem, and a fresh catalyst was used for each test. As indicated in Figure 4, at 500 °C, H-LIF concentrations above the PtMn are comparable to those of the noncatalytic materials, within uncertainties. This observation suggests that there are not significant amounts of H atoms desorbed from the catalyst and transported short, localized distances (50−300 μm) away from the surface, despite H being known to form on the surface.[31] At 700 °C, H-LIF above the catalyst does not increase significantly (unlike quartz and steel), and H-LIF is noticeably lower than either noncatalytic surface, which again mirrors the reduced bulk dehydrogenation performance of the catalysts at elevated temperatures. It is worth noting that since H production over quartz is expected to be driven by thermal pyrolysis of ethane, even if the catalyst was completely deactivated at this temperature, one might expect the thermal production of H would be the same as that of the quartz. The observation of reduced concentrations of H over PtMn suggests the catalyst acts more as a H sink rather than source for gas-phase H.

As coking and deactivation is a known problem for dehydrogenation catalysts, the temporal response of the PtMn catalyst was also measured, and the results are shown in Figure 5. For these experiments, a freshly reduced catalyst was heated to the desired temperature in pure nitrogen. Once ethane was introduced to the reactant stream, LIF measurements are made every few minutes. Measurements for each data point take 1−2 min. H concentrations are comparable in the first 2 min of ethane introduction at both 500 and 700 °C. Notably, the concentration of H over the PtMn surface drastically drops within minutes. While the measured H-LIF reduces significantly over the course of an hour at both 500 and 700 °C, the reduction is much faster at 700 °C. These rapid changes in local chemical composition highlight one of the challenges of catalytic dehydrogenation. In principle, the reduction in H could be due to reduced gas temperatures, changes in local mass transport, or changes in surface activity. It is unlikely that the surface temperature will change significantly enough to cause the observed reduction in H, and mass transport near the surface will be dominated by the fixed flow conditions and should not change. Therefore, the observed changes are reasonably attributed to changes in surface activity. This change in activity likely includes significant coking of the catalyst at this temperature and may include increased adsorption/absorption of H in the "H-sink" mentioned above, though the mechanism is uncertain. Clearly, however, these results confirm that PtMn is not as effective at higher temperatures. Reduction of H-LIF to negligible quantities after 60 min also precludes the possibility that H is being photolytically produced in the reactants in these experiments.

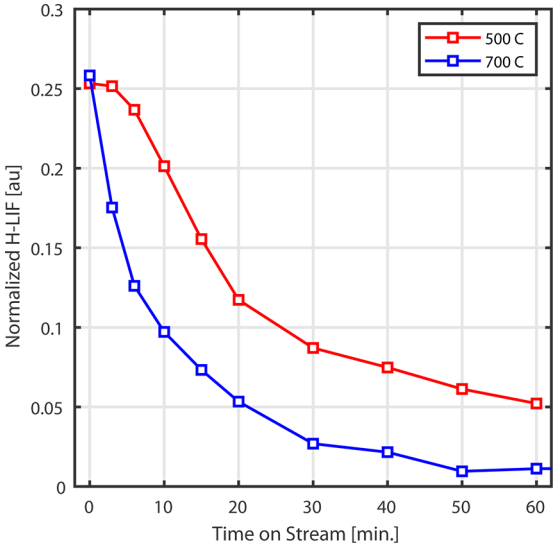

Figure 5. Temporal profiles of H-LIF over PtMn catalyst at 500 and 700 °C.

One key virtue of this characterization technique is the ability to locally assess reaction activity as a function of distance from the heated surface. Figure 6 shows these results

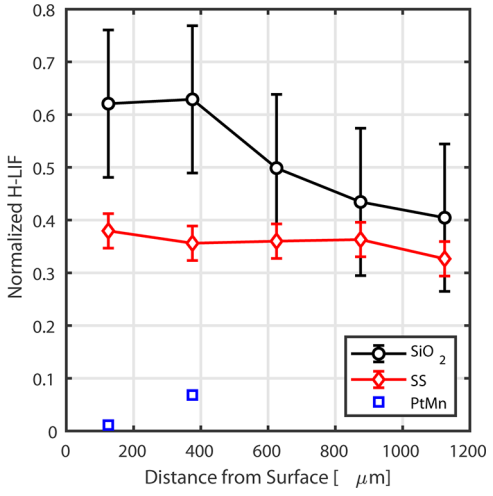

Figure 6. Normalized H-LIF above quartz, stainless steel, and PtMn catalyst at 700 °C. Data for PtMn at 125 and 375 μm are taken 60 and 62 min after ethane introduction, respectively.

for all three materials at 700 °C. For quartz, H-LIF remains high near the surface (within 400 μm) before dropping off gradually by about 35% 1 mm from the surface. As H production over this inert surface is driven by gas-phase reactions, the H-LIF profile suggests a gradual reduction in gas temperature going away from the surface, as would be expected. Interestingly, H-LIF over steel remains more consistent, dropping by about 15% over 1 mm, though starting at a lower amount. The convergence in H-LIF between quartz and steel over 800 μm from the surface may be representative of a consistent gas-phase temperature at this distance. The

https://doi.org/10.1021/acs.jpcc.1c09955
J. Phys. Chem. C 2022, 126, 3054−3059

lower concentration of H near the surface of steel, relative to quartz, then indicates surface chemistry that inhibits formation of H or consumes H. Steel surfaces have been shown to promote radical recombination within a few mm in reacting flows.[41] More interestingly, H-LIF over PtMn increases at an increased distance from the surface. Figure 6 shows measured H-LIF 125 μm from PtMn after 1 h, where the signal has dropped to negligible levels. However, probing 375 μm away from the surface 2 min later shows higher levels of H. This observation indicates that the surface inhibition or consumption effect is even stronger on the catalytic surface. Though consumption of H through radical recombination may occur near the surface, reduced formation of H is also expected based on the observed reduced dehydrogenation performance.[28] Gas-phase temperature measurements are necessary to determine the extent to which the surfaces affect the local temperature field. However, these highly localized observations provide new insights into the possible mechanisms behind the observed differences in dehydrogenation efficiency above these varied surfaces and are uniquely identified by H-LIF studies.

4. CONCLUSIONS

This report details the first near-catalyst gas-phase hydrogen atom measurements by laser-induced fluorescence. Local hydrogen atom measurements above heated quartz, stainless steel, and PtMn-based catalyst in an ethane/nitrogen stagnation flow between room temperature and 700 °C showed hydrogen concentrations above quartz were higher than steel or PtMn with the difference in concentration more significant at higher temperatures. Using H atom as a reporter of ethane dehydrogenation, the results are consistent with previously observed superior performance of quartz as an ethane dehydrogenation reactor material.[28] Local LIF measurements provide new insights about the possible mechanisms behind these differences. In particular, surface chemistry that inhibits H formation or increases H consumption, may alter dehydrogenation chemical pathways. Meanwhile, rapid catalyst deactivation from coking or H consumption by PtMn catalyst appears to diminish H concentrations locally above the surface. This study exemplifies the potential value of highly localized, surface-specific measurements of gas reaction chemistry enabled by H-LIF spectroscopy.

AUTHOR INFORMATION

Corresponding Authors

Erik D. Spoerke − *Sandia National Laboratories, Albuquerque, New Mexico 871845, United States;* orcid.org/0000-0003-2286-2560; Email: edspoer@sandia.gov

Christopher J. Kliewer − *Combustion Research Facility, Sandia National Laboratories, Livermore, California 94551, United States*; Email: cjkliew@sandia.gov

Authors

Scott A. Steinmetz − *Combustion Research Facility, Sandia National Laboratories, Livermore, California 94551, United States;* orcid.org/0000-0003-1101-4662

Andrew T. DeLaRiva − *Department of Chemical and Biological Engineering and Center for Microengineering Materials, University of New Mexico, Albuquerque, New Mexico 87131, United States*

Christopher Riley − *Sandia National Laboratories, Albuquerque, New Mexico 871845, United States;* orcid.org/0000-0002-6403-0677

Paul Schrader − *Combustion Research Facility, Sandia National Laboratories, Livermore, California 94551, United States*

Abhaya Datye − *Department of Chemical and Biological Engineering and Center for Microengineering Materials, University of New Mexico, Albuquerque, New Mexico 87131, United States;* orcid.org/0000-0002-7126-8659

Complete contact information is available at: https://pubs.acs.org/10.1021/acs.jpcc.1c09955

Notes

The authors declare no competing financial interest.

ACKNOWLEDGMENTS

This work was supported by the U.S. Department of Energy's Office of Energy Efficiency and Renewable Energy (EERE), under the Advanced Manufacturing Office, FOA Number DE-LC 000L059. C.J.K. acknowledges support by the U.S. Department of Energy (DOE), Office of Basic Energy Sciences (BES), Division of Chemical Sciences, Geosciences and Biosciences under FWP 021507 for the development of the near-surface gas-phase femtosecond TALIF approach. This work was performed, in part, at the Center for Integrated Nanotechnologies, an Office of Science User Facility operated for the U.S. Department of Energy (DOE) Office of Science. Sandia National Laboratories is a multimission laboratory managed and operated by National Technology and Engineering Solutions of Sandia, LLC, a wholly owned subsidiary of Honeywell International, Inc., for the U.S. DOE's National Nuclear Security Administration under Contract DE-NA0003525. The views expressed in this Article do not necessarily represent the views of the U.S. DOE or the United States Government. Catalyst synthesis and characterization at the University of New Mexico was supported by the NSF/ERC CISTAR, which is supported by the National Science Foundation under Cooperative Agreement No. EEC-1647722. The authors thank Brian Patterson for technical assistance.

REFERENCES

(1) Vincent, R. S.; Lindstedt, R. P.; Malik, N. A.; Reid, I. A. B.; Messenger, B. E. The Chemistry of Ethane Dehydrogenation over a Supported Platinum Catalyst. *J. Catal.* **2008**, *260*, 37−64.

(2) Rupprechter, G.; Weilach, C. Spectroscopic Studies of Surface-Gas Interactions and Catalyst Restructuring at Ambient Pressure: Mind the Gap! *J. Phys.: Condens. Matter* **2008**, *20*, 184019.

(3) Chakrabarti, A.; Ford, M. E.; Gregory, D.; Hu, R.; Keturakis, C. J.; Lwin, S.; Tang, Y.; Yang, Z.; Zhu, M.; Bañares, M. A.; Wachs, I. E. A Decade+ of Operando Spectroscopy Studies. *Catal. Today* **2017**, *283*, 27−53.

(4) Fridell, E.; Westblom, U.; Aldén, M.; Rosén, A. Spatially Resolved Laser-Induced Fluorescence Imaging of OH Produced in the Oxidation of Hydrogen on Platinum. *J. Catal.* **1991**, *128*, 92−98.

(5) Fridell, E.; Elg, A. P.; Rosén, A.; Kasemo, B. A Laser-Induced Fluorescence Study of OH Desorption from Pt(111) during Oxidation of Hydrogen in O2 and Decomposition of Water. *J. Chem. Phys.* **1995**, *102*, 5827−5835.

(6) Gudmundson, F.; Persson, J. L.; Forsth, M.; Behrendt, F.; Kasemo, B.; Rosén, A. OH Gas Phase Chemistry Outside a Pt Catalyst. *J. Catal.* **1998**, *179*, 420−430.

(7) Försth, M.; Gudmundson, F.; Persson, J. L.; Rosén, A. The Influence of a Catalytic Surface on the Gas-Phase Combustion of H_2 + O_2. *Combust. Flame* **1999**, *119*, 144−153.
(8) Gudmundson, F.; Fridell, E.; Rosén, A.; Kasemo, B. Evaluation of OH Desorption Rates from Pt Using Spatially Resolved Imaging of Laser-Induced Fluorescence. *J. Phys. Chem.* **1993**, *97*, 12828−12834.
(9) Zetterberg, J.; Blomberg, S.; Gustafson, J.; Sun, Z. W.; Li, Z. S.; Lundgren, E.; Aldén, M. An in Situ Set up for the Detection of CO2 from Catalytic CO Oxidation by Using Planar Laser-Induced Fluorescence. *Rev. Sci. Instrum.* **2012**, *83*, 053104.
(10) Zetterberg, J.; Blomberg, S.; Gustafson, J.; Evertsson, J.; Zhou, J.; Adams, E. C.; Carlsson, P.-A.; Aldén, M.; Lundgren, E. Spatially and Temporally Resolved Gas Distributions around Heterogeneous Catalysts Using Infrared Planar Laser-Induced Fluorescence. *Nat. Commun.* **2015**, *6*, 7076.
(11) Zhou, J.; Matera, S.; Pfaff, S.; Blomberg, S.; Lundgren, E.; Zetterberg, J. Combining Planar Laser-Induced Fluorescence with Stagnation Point Flows for Small Single-Crystal Model Catalysts: CO Oxidation on a Pd(100). *Catalysts* **2019**, *9*, 484.
(12) Pfaff, S.; Zhou, J.; Hejral, U.; Gustafson, J.; Shipilin, M.; Albertin, S.; Blomberg, S.; Gutowski, O.; Dippel, A.; Lundgren, E.; Zetterberg, J. Combining High-Energy X-Ray Diffraction with Surface Optical Reflectance and Planar Laser Induced Fluorescence for Operando Catalyst Surface Characterization. *Rev. Sci. Instrum.* **2019**, *90*, 033703.
(13) Blomberg, S.; Brackmann, C.; Gustafson, J.; Aldén, M.; Lundgren, E.; Zetterberg, J. Real-Time Gas-Phase Imaging over a Pd(110) Catalyst during CO Oxidation by Means of Planar Laser-Induced Fluorescence. *ACS Catal.* **2015**, *5*, 2028−2034.
(14) Matera, S.; Blomberg, S.; Hoffmann, M. J.; Zetterberg, J.; Gustafson, J.; Lundgren, E.; Reuter, K. Evidence for the Active Phase of Heterogeneous Catalysts through In Situ Reaction Product Imaging and Multiscale Modeling. *ACS Catal.* **2015**, *5*, 4514−4518.
(15) Blomberg, S.; Zetterberg, J.; Gustafson, J.; Zhou, J.; Brackmann, C.; Lundgren, E. Comparison of AP-XPS and PLIF Measurements during CO Oxidation over Pd Single Crystals. *Top. Catal.* **2016**, *59*, 478−486.
(16) Blomberg, S.; Zhou, J.; Gustafson, J.; Zetterberg, J.; Lundgren, E. 2D and 3D Imaging of the Gas Phase Close to an Operating Model Catalyst by Planar Laser Induced Fluorescence. *J. Phys.: Condens. Matter* **2016**, *28*, 453002.
(17) Blomberg, S.; Zetterberg, J.; Zhou, J.; Merte, L. R.; Gustafson, J.; Shipilin, M.; Trinchero, A.; Miccio, L. A.; Magaña, A.; Ilyn, M.; Schiller, F.; Ortega, J. E.; Bertram, F.; Grönbeck, H.; Lundgren, E. Strain Dependent Light-off Temperature in Catalysis Revealed by Planar Laser-Induced Fluorescence. *ACS Catal.* **2017**, *7*, 110−114.
(18) Lundgren, E.; Zhang, C.; Merte, L. R.; Shipilin, M.; Blomberg, S.; Hejral, U.; Zhou, J.; Zetterberg, J.; Gustafson, J. Novel in Situ Techniques for Studies of Model Catalysts. *Acc. Chem. Res.* **2017**, *50*, 2326−2333.
(19) Zhou, J.; Blomberg, S.; Gustafson, J.; Lundgren, E.; Zetterberg, J. Simultaneous Imaging of Gas Phase over and Surface Reflectance of a Pd(100) Single Crystal during CO Oxidation. *J. Phys. Chem. C* **2017**, *121*, 23511−23519.
(20) Zhou, J.; Blomberg, S.; Gustafson, J.; Lundgren, E.; Zetterberg, J. Visualization of Gas Distribution in a Model AP-XPS Reactor by PLIF: CO Oxidation over a Pd(100) Catalyst. *Catalysts* **2017**, *7*, 29.
(21) Karakaya, C.; Deutschmann, O. Kinetics of Hydrogen Oxidation on Rh/Al_2O_3 Catalysts Studied in a Stagnation-Flow Reactor. *Chem. Eng. Sci.* **2013**, *89*, 171−184.
(22) Zellner, A.; Suntz, R.; Deutschmann, O. Two-Dimensional Spatial Resolution of Concentration Profiles in Catalytic Reactors by Planar Laser-Induced Fluorescence: NO Reduction over Diesel Oxidation Catalysts. *Angew. Chemie - Int. Ed.* **2015**, *54*, 2653−2655.
(23) Wan, S.; Torkashvand, B.; Häber, T.; Suntz, R.; Deutschmann, O. Investigation of HCHO Catalytic Oxidation over Platinum Using Planar Laser-Induced Fluorescence. *Appl. Catal. B Environ.* **2020**, *264*, 118473.
(24) Zhou, B.; Huang, E.; Almeida, R.; Gurses, S.; Ungar, A.; Zetterberg, J.; Kulkarni, A.; Kronawitter, C. X.; Osborn, D. L.; Hansen, N.; Frank, J. H. Near-Surface Imaging of the Multicomponent Gas Phase above a Silver Catalyst during Partial Oxidation of Methanol. *ACS Catal.* **2021**, *11*, 155−168.
(25) Sattler, J. J. H. B.; Ruiz-Martinez, J.; Santillan-Jimenez, E.; Weckhuysen, B. M. Catalytic Dehydrogenation of Light Alkanes on Metals and Metal Oxides. *Chem. Rev.* **2014**, *114*, 10613−10653.
(26) Li, C.; Wang, G. Dehydrogenation of Light Alkanes to Mono-Olefins. *Chem. Soc. Rev.* **2021**, *50*, 4359−4381.
(27) Amghizar, I.; Vandewalle, L. A.; Van Geem, K. M.; Marin, G. B. New Trends in Olefin Production. *Engineering* **2017**, *3*, 171−178.
(28) Riley, C. R.; De La Riva, A.; Ibarra, I. L.; Datye, A. K.; Chou, S. S. Achieving High Ethylene Yield in Non-Oxidative Ethane Dehydrogenation. *Appl. Catal. A Gen.* **2021**, *624*, 118309.
(29) Quinn, C. P. The Thermal Dissociation and Pyrolysis of Ethane. *Proc. R. Soc. A* **1963**, *275*, 190−199.
(30) Xu, C.; Al Shoaibi, A. S.; Wang, C.; Carstensen, H. H.; Dean, A. M. Kinetic Modeling of Ethane Pyrolysis at High Conversion. *J. Phys. Chem. A* **2011**, *115*, 10470−10490.
(31) Prins, R. Hydrogen Spillover. Facts and Fiction. *Chem. Rev.* **2012**, *112*, 2714−2738.
(32) Baumgarten, E.; Lentes-Wagner, C.; Wagner, R. Hydrogen Spillover through Gas Phase Transport of Hydrogen Atoms. *J. Catal.* **1989**, *117*, 533−541.
(33) Baumgarten, E.; Krupp, R. Gas Phase Hydrogen Spillover and Oxygen Content. *React. Kinet. Catal. Lett.* **2000**, *70*, 27−33.
(34) Baumgarten, E.; Krupp, R. Hydrogenation of Hexene-1 by Gas Phase Spillover Hydrogen. Influence of Substance Added in the Reaction Chamber, without Contact to the Catalyst. *React. Kinet. Catal. Lett.* **2000**, *70*, 35−41.
(35) Baumgarten, E.; Maschke, L. Hydrogen Spillover through the Gas Phase. Reaction with Graphite and Activated Carbon. *Appl. Catal. A Gen.* **2000**, *202*, 171−177.
(36) Baumgarten, E.; Meyer, G. Hydrogen Spillover through the Gas Phase. Some Kinetic Aspects. *React. Kinet. Catal. Lett.* **2000**, *71*, 325−333.
(37) Baumgarten, E.; Meyer, G. Indirect Catalysis, Caused by Hydrogen Spillover through the Gas Phase. Activation by Hydrogen Oxygen Reaction. *React. Kinet. Catal. Lett.* **2000**, *71*, 335−341.
(38) Wu, Z.; Bukowski, B. C.; Li, Z.; Milligan, C.; Zhou, L.; Ma, T.; Wu, Y.; Ren, Y.; Ribeiro, F. H.; Delgass, W. N.; Greeley, J.; Zhang, G.; Miller, J. T. Changes in Catalytic and Adsorptive Properties of 2 Nm Pt3Mn Nanoparticles by Subsurface Atoms. *J. Am. Chem. Soc.* **2018**, *140*, 14870−14877.
(39) Jain, A.; Wang, Y.; Kulatilaka, W. D. Three-Photon-Excited Laser-Induced Fluorescence Detection of Atomic Hydrogen in Flames. *Opt. Lett.* **2019**, *44*, 5945−5948.
(40) Schmidt, J. B.; Roy, S.; Kulatilaka, W. D.; Shkurenkov, I.; Adamovich, I. V.; Lempert, W. R.; Gord, J. R. Femtosecond, Two-Photon-Absorption, Laser-Induced-Fluorescence (Fs-TALIF) Imaging of Atomic Hydrogen and Oxygen in Non-Equilibrium Plasmas. *J. Phys. D. Appl. Phys.* **2017**, *50*, 015204.
(41) Yang, H.; Feng, Y.; Wu, Y.; Wang, X.; Jiang, L.; Zhao, D.; Yamashita, H. A Surface Analysis-Based Investigation of the Effect of Wall Materials on Flame Quenching. *Combust. Sci. Technol.* **2011**, *183*, 444−458.

https://doi.org/10.1021/acs.jpcc.1c09955
J. Phys. Chem. C 2022, 126, 3054−3059